

CONSIGLIO NAZIONALE DELLE RICERCHE

**RESONANCE PHENOMENA ACCOMPANYING
THE INJECTION OF A PERIODICALLY
PULSED NEUTRAL BEAM INTO A TOKAMAK**

D. Farina, R. Pozzoli, D. Ryutov

FP 92/18

November 1992

ISTITUTO DI FISICA DEL PLASMA
ASSOCIAZIONE EURATOM-ENEA-CNR

20133 Milano (Italy) - Via Bassini,15

**RESONANCE PHENOMENA ACCOMPANYING THE INJECTION
OF A PERIODICALLY PULSED NEUTRAL BEAM
INTO A TOKAMAK**

D.Farina

Istituto di Fisica del Plasma, C.N.R., Milano, Italy,

R.Pozzoli

Dipartimento di Fisica, Università di Milano, Milano, Italy,

D.Ryutov

Budker Institute of Nuclear Physics, Novosibirsk, Russia

ABSTRACT

The paper considers the temporal behaviour of fast ions produced in a tokamak plasma by the injection of a periodically pulsed neutral beam. It is shown that, if the temporal distance between the pulses is properly chosen, then a dense bunch of fast ions is formed near a certain resonant magnetic surface. Temporal and spatial behaviour of these bunches is studied in some detail for the simple model of a large aspect ratio tokamak. Possible diagnostics implications of this phenomenon are discussed.

1. INTRODUCTION

During the past decade, the neutral beam (NB) technology has made a remarkable progress, in particular, for diagnostics applications. The survey of recent achievements in this field can be found, e.g., in papers /1,2/.

In the present paper, we discuss one more possible application of neutral beam technique: we show that injection of a periodically pulsed neutral beam into a tokamak plasma can give rise to interesting resonance phenomena which can be of some importance for the plasma diagnostics and other purposes.

We consider only relatively weak beams which do not perturb the plasma parameters, and study the evolution of the population of thus produced fast particles in the given plasma background. Bearing in mind that, for the fast ions, the transit time is by several orders of magnitude shorter than any of the collision times, we neglect the collisions of the fast ions with plasma particles.

To gain some insight on the kind of resonances that can be expected in such a system, let us consider the particles that are trapped near some rational flux surface, where the field line gets closed after, say, m turns in a toroidal direction θ and n turns in a poloidal direction ϕ . Let us denote the transit time of the fast particles along the field line as T_{mn} . If the separation T between neutral beam pulses (Fig.1) is just equal to T_{mn} , then the successive pulses will be added to each other, with exact overlapping of their positions in space and time. For large enough number N of the pulses in the pack, this will result in the build-up of a large amplitude bunch of fast ions, whose density should be considerably higher than the density of each single pulse. This bunch will move around the tokamak, producing a pulsed periodic perturbations on all kinds of the diagnostics monitors.

If, on the other hand, we consider surfaces separated by some distance from the resonant one, the effect of "stacking" of the successive pulses gradually disappears with increasing separation and, finally, at large enough separation, the density variation acquires a stochastic character. The same happens also if T differs from the resonant period T_{mn} .

The fact that the particles trapped from the external source behave differently on the resonant surfaces has already been observed experimentally, in the studies of pellet injection /3/. In our problem, the periodicity of the source and the presence of well defined temporal resonances arising from the fact that NB can provide the ions with a small velocity spread (and, correspondingly, with well defined transit frequency) add a new dimension to the whole phenomenon.

In principle, this phenomenon can be used for diagnostics purposes, providing a more detailed information on the structure of magnetic field (from studying the locations of the resonances) and also on the effect of plasma fluctuations on the fast ions (from the width of the resonances). It is appropriate to mention here that the possibility of using the neutral beams (though quasistationary ones, without employing the resonance phenomena) for magnetic field measurements has been considered some time ago by Jobes /4/. This interesting proposal has been already realised experimentally on the TUMAN device /5/.

The present paper had not been intended to provide any self-consistent proposal of a diagnostics on any of the particular devices, as this could be done only with a thorough account of concrete experimental environment of the machines. We were rather intending to present a general description of the phenomenon and thus to give a necessary initial information for the possible further analysis.

The structure of the resonances can be understood particularly easily for large aspect ratio tokamaks, where the variation of the toroidal magnetic field over the minor radius can be neglected (the "cylindrical model" of a tokamak, see e.g. Ref. 6). The corresponding analysis is presented in Sec.2 for the reference case of the beam of zero transverse dimensions and zero angular and velocity spread. Some estimates of the possible role of the finite beam brightness are presented in Sec.3. In Sec.4, new elements that can be brought about by finite toroidicity effects, are mentioned. Numerical estimates related to possible diagnostics applications are presented in Sec.5. Summary of the results is given in Sec.6.

2. RESONANCES IN A CYLINDRICAL TOKAMAK

2.1 Description of the model

The model we are considering in the present paper, is illustrated by Fig.2: a tokamak is replaced by a cylinder, with the understanding that the sections separated by the distance

$$L = 2\pi R \quad (1)$$

where R denotes the major radius, should be considered as identical ones. We use the cylindrical coordinate system (r, ϕ, z) ; sometimes, it is more convenient to replace z by an analogue of the toroidal angle

$$\theta = z/R \quad (2)$$

The toroidal magnetic field B_z in our approximation is just uniform. To characterize the poloidal field B_ϕ , we use a description in terms of the safety factor $q(r)$:

$$B_\phi = B_z [r/Rq(r)] \quad (3)$$

The equations of the magnetic field line that intersects the plane $\theta = 0$ at some point $r = r_0, \phi = \phi_0$, are:

$$r = r_0, \quad \phi = \phi_0 + \theta/q(r) \quad (4)$$

Let us assume that the beam has vanishingly small transverse dimensions and is aimed to the tokamak axis (Fig.2). Let α be the angle between the tokamak axis and direction of the beam injection. Then, if a beam particle is trapped on a certain radius r , a fast particle is produced whose parallel (with respect to the magnetic field) component of velocity is determined by the expression:

$$v_{\parallel} = v \cos \alpha (1 + r^2/q^2 R^2)^{-1/2} \quad (5)$$

As in the cylindrical geometry the magnetic field strength does not change along the field line, v_{\parallel} does not depend on time. The projections of the parallel velocity on the unit vectors corresponding to z and ϕ co-ordinates, are:

$$v_z = v_{\parallel} (1 + r^2/q^2 R^2)^{-1/2}, \quad v_{\phi} = v_{\parallel} (r/qR) (1 + r^2/q^2 R^2)^{-1/2} \quad (6)$$

We neglect the finite gyroradius effects and consider a Larmor circle just as a point. The angular frequencies of rotation of the particle guiding centre in the toroidal and poloidal directions are then

$$\Omega(r) = v_z/R \quad (7)$$

and

$$\omega(r) = v_{\phi}/r = \Omega(r)/q(r), \quad (8)$$

respectively.

In the cylindrical geometry, the radius r of the particle trajectory is a constant of motion. Correspondingly, the equations that determine the positions of the ions at $t > 0$ can be written as:

$$\theta = \Omega(r) t + \theta_0, \quad \phi = \omega(r) t + \phi_0, \quad r = r_0 \quad (9)$$

Note that in the model of a large aspect ratio tokamak v_z and Ω are almost independent of r . We, however, will not use this fact, in order to be able to reach some understanding of the situation in tokamaks with finite aspect ratio where the variation of Ω over the minor radius can be considerable. On the other hand, we will exploit the smallness of the parameter r/R in two other respects. Firstly, we neglect a small delay in the moments of the NB particles trapping caused by their finite flight-time over the minor radius. Secondly, we neglect some differences in the positions of particles in z - direction in the moment of trapping (which is a result of the skew injection of the beam).

One can show (see Appendix 1) that appropriate account for these two effects indeed gives only small corrections to the effects discussed in our paper.

2.2 Stacking of the bunches

For the moment, we assume that the pulses have an infinitely short duration, $\tau = 0$. When the first such a pulse is just trapped, the fast ions occupy one of the device diameters:

$$\theta = 0, \quad \phi = 0, \quad 0 < r < a \quad (10a)$$

and

$$\theta = 0, \quad \phi = \pi, \quad 0 < r < a \quad (10b)$$

The relationships (10b) describe the ions that are trapped at the opposite (with respect to injection point) side from the axis. It is clear that, if we will know the motion of the particles trapped before the axis, then the motion of those trapped behind the axis will be essentially the same, just with the shift of π over the variable ϕ . Accordingly, we consider now only the motion of the ions trapped before the axis.

At any instant of time, the Eqs. (9) determine the line, to which the initial straight segment (10a) is transformed. For given dependences of $\Omega(r)$ and $\omega(r)$, one can eliminate r from equations (9) and find the projection of this line to the (θ, ϕ) plane.

For definiteness, we consider the case when both $\Omega(r)$ and $\omega(r)$ are positive, with $\Omega(0) < \omega(0)$ (i.e., $q < 1$ on the axis), and with Ω and ω decreasing radially in a way that, at a certain intermediate radius, Ω becomes equal to ω (i.e., the condition $q = 1$ is satisfied there) while at larger radii Ω exceeds ω . The illustration of this kind of dependences is given on Fig.3. They are representative for a broad class of tokamak discharges (see, e.g., /7/).

The interval of variation of θ at any instant $t = const$ is determined by the values $\Omega(0)t$ and $\Omega(a)t$. The plot of ϕ versus θ for subsequent instants of time is shown in

Fig.4a. Note that at $t = 0$, the stretch (10a) is projected in the (θ, ϕ) plane just to the point $\theta = \phi = 0$. The diagonal $\phi = \theta$ corresponds to the radius where $q = 1$. The upper and lower points of every stretch correspond to the axis ($r = 0$) and edge ($r = a$), respectively. As soon as maximum value of ϕ or θ exceeds 2π , the corresponding section of the line should be displaced by 2π downwards and appears again inside the square $0 < \phi < 2\pi$, $0 < \theta < 2\pi$ (see, for example, curves (d) and (e) on Fig.4a). At large enough times the picture acquires the form shown in Fig.4b.

Now we consider the same picture for the sequence of several bunches, under the condition of an exact resonance at $q = 1$ surface ($T = T_{11}$). When the second bunch arrives, the first has the form shown by the curve (e) on Fig. 4a. In the subsequent moments, the second bunch repeats the evolution of the first, with the point of intersection of both bunches with $\theta = \phi$ diagonal coinciding all the time. For illustration, the curves for the moments $t = 1.5 T$ and $t = 2.5 T$ (when the third bunch has already arrived), are shown in Fig.4c and 4d. Note, that the curves from the successive bunches gradually diverge with growing distance from the resonant point. The later bunches are directly superimposed on the earlier ones only for the case when both Ω and ω depend on r linearly.

Also instructive is the counting of intersections of the stretch (10a) from the first bunch with some minor cross-section of the tokamak, $\theta = \text{const}$. At $t \gtrsim T$, the number of intersections scales, roughly speaking, as t/T . After $M \gg 1$ periods, the number of intersections is within the order of magnitude equal to M . The intersections from the subsequent pulses also appear on the picture. Just after injection of the last (N -th) pulse, the number of intersections roughly equals to $N^2/2$. At longer times ($t > NT$) the number of intersections grows linearly (Nt/T).

The stacking effect occurs not only at $T = T_{mn}$ but also in the cases when T/T_{mn} is a rational number. For instance, if $T = 2T_{mn}$, the adding of the next pulse occurs after two (not one) revolutions of the previous pulse; if $T = T_{mn}/2$, two groups of resonant bunches are formed. However, the most efficient stacking occurs just at $T = T_{mn}$.

The object that is formed by resonant stacking of the bunches has a small cross-section (determined by the finite pulse-length and finite transverse dimensions of the neutral beam - effects that will be discussed later) and a relatively large longitudinal extent. In order to avoid possible misunderstandings, we emphasize that it does not coincide with any of the field lines: from what has been said above, it is clear that it intersects the magnetic surfaces, and if we consider its intersection point with a certain magnetic surface its projection on this surface in the vicinity of the intersection point forms a finite angle with the field-line passing through this point. In this - as well as in many other - respects the object under study is very different from the "snake" phenomenon /3/. We propose to call this object "tagliatella" - for the close resemblance of its shape to that of the one of the kinds of Italian noodles.

2.3 Detection of the resonances

One of possible ways of detecting the formation of the resonant bunches is a measurement of the line-density of the fast particles in one of the tokamak cross-sections. In principle, this could be done by using one more neutral beam, that would provide a charge-exchange target for fast particles, and observing the thus formed charge-exchange neutrals escaping from the plasma along a given direction. Let the transverse dimensions of the sampling volume be ζ in z - direction, and η in the direction transverse to both z and the line of sight; let d be the displacement of the line of sight with respect to the device axis (Fig. 5). For a large aspect ratio tokamak, at the comparable values of ζ and η , the angular width of the sampling volume in θ ($\Delta\theta \sim \zeta/R$) is much smaller than the angular width in ϕ ($\Delta\phi \sim \eta/r$).

We assume that the monitor counts the number of particles in the sampling volume, i.e., the total length of the stretches intersecting this volume, with a proper weight ascribed to the every stretch (the number of particles per unit length of the line occupied by the injected particles at a given instant of time). Of course, in a real experiment the way of counting and the weighting procedure may be somewhat different but this will not affect the essence of the analysis that follows.

2.4 Numerical model

The numerical evaluation of the signals from the sampling volume is based on the analysis of the temporal evolution of the initial stretches (10a). The intersections of the tagliatella with the sampling volume are numerically monitored, and the weights ascribed to every intersection are computed according to Eq.(A2.6) of Appendix 2. All the simultaneous intersections are then summed up with appropriate weight to give an expected signal S from the sampling volume (from what has been stated, it is clear that we identify the signal with the total number of fast ions simultaneously present in the sampling volume).

As our calculations are of a model nature, we have chosen the function $f(r)$ (that describes the spatial distribution of the initially trapped ions, see Appendix 2) just as a constant, with a "hole" near the axis:

$$f(r) = \begin{cases} \text{const}, & a_1 < r < a \\ 0, & r < a_1 \end{cases}$$

The hole simulates the attenuation of the neutral beam approaching the axis of the device. For simplicity, we neglect term of order r^2 in the expression (A2.6). Then, for the chosen linear model for the $\Omega(r)$ dependence, the weighting factor is just constant at $r > a_1$, and zero at $r < a_1$. These assumptions have been used in the derivation of the numerical results throughout the rest of the paper.

2.5 Case of exact resonance

For definiteness, we refer to the $q = 1$ resonance, for which the resonant period is T_{11} . Let us first analyze the statistics of the countings from the first bunch, at the moment $t \sim MT_{11}$ when there are M intersections. The number of crossings with the sampling volume depends on its width η : if η/a exceeds $1/M$, then there are several crossings ($\approx M\eta/a$), and the signal is relatively smooth, with the average level proportional to η and the relative fluctuation level with respect to the average one of the order of $(M\eta/a)^{-1/2}$.

If, on the contrary, η is smaller than a/M , then the signal consists of the separate spikes of the length $\Delta\phi T_{11}/2\pi$ separated by empty periods of the order of T_{11}/M .

Denoting the total number of particles trapped from the single NB pulse by P , we can say that at the time $t > T/2$, the number of the particles per unit length of the tagliatella roughly equals PT/Lt (Cf. Appendix 2). Accordingly, the average number of particles in the sampling volume equals to $(PT/t)(\Delta\theta/2\pi)(M\eta/a)$ at $\eta > a/M$; the number of particles in a separate pulse is equal to $(PT/t)(\Delta\theta/2\pi)$ at $\eta < a/M$. These qualitative conclusions are supported by the numerical results presented in Fig.6.

The same consideration allows to evaluate the linear density of the tagliatella near the point of exact resonance after stacking $M < N$ pulses: the linear density should be obtained by summation over subsequent pulses. If the time t is not very close to the moment when the last (M -th) pulse had been injected, i.e., $|t - MT| \gtrsim T_{11}/2$, then the sum is approximately equal to

$$(P/L) \ln M. \quad (11)$$

The exact expression is presented in Appendix 2. If this resonant bunch crosses the sampling volume, it produces the signal which has a height of

$$P(\Delta\theta/2\pi) \ln M. \quad (12)$$

Of course, to observe this big signal, one should properly position the sampling volume (so that it would cross the line $\theta = \phi$). The duration of the signal from the resonant bunch is then equal to

$$(T/2\pi)(\eta/a) \approx T(\Delta\phi/2\pi), \quad (13)$$

unless the line of sight is almost tangent to the $q = 1$ surface. The latter case can also be easily analyzed, but we will not present here the corresponding simple calculations.

Now, we are prepared to present the overall picture of the signal collected from the sampling volume shown in Fig.5 in the case when it intersects the resonant field line

$\theta = \phi$. First, we see the spikes corresponding to the $q = 1$ surface; the height of these spikes grows logarithmically with the number of pulses injected, reaching the value of

$$P(\Delta\theta/2\pi) \ln N \quad (14)$$

at $t \simeq NT_{11}$. After the last pulse has been injected, the height of the resonant spikes decreases due to the decreasing linear density (see Appendix 2): at $T/2 \lesssim t - NT \lesssim NT$ as $\ln[NT/(t - NT)]$, and at $t \gtrsim 2NT$ as $1/t$.

Superimposed on these spikes, are signals from "non-resonant" particles (not belonging to the $q = 1$ surface), crossing the sampling volume. The character of this background signal changes with time: from a sporadic, consisting of well separated spikes during the injection of the first few bunches, to a quasicontinuous at later phases.

The behaviour of the signal described above is shown in Fig.7, where it is also compared with the given analytical estimates for the envelope of resonant pulses.

In the time interval following the injection of the last NB bunch, a considerable continuous signal will be formed, if the sampling volume is not too narrow, i.e., for

$$\eta/a \gg 2\pi/N^2. \quad (15)$$

This signal comes from the bunches that have been injected not too close to the observation time, $N - m > (a/\eta)^{1/2}$, where $m = 0$ corresponds to the last pulse. The particles from these bunches can be considered as uniformly distributed over the volume of tokamak. Their number in the sampling volume can be evaluated as

$$NP(\eta/a)(\Delta\theta/2\pi) \quad (16)$$

From comparison of the evaluations (14) and (16) it is clear that to have the resonant spikes much higher than the background, one should choose η to be sufficiently small

$$(\eta/a) \ll \ln N/N. \quad (17)$$

We will assume that the even more stringent inequality

$$(\eta/a) \lesssim 1/N \quad (18)$$

is satisfied. The further reduction of η is, probably, undesirable: as we shall see below, with the account of the finite pulse-width and velocity spread this may cause the undesirable reduction of the useful signal.

2.6 Effect of the frequency mismatch and of the line-of-sight displacement

Now we consider the effect of small deviation ΔT of the injection period from the resonant value T_{11} . If the mismatch ΔT is smaller than $T\Delta\phi/2\pi N$, then it has virtually no effect on the pulse-shape, as all the bunches still can be simultaneously covered by the sampling volume. At

$$\Delta\phi/2\pi N \lesssim \Delta T/T \lesssim \Delta\phi/2\pi \quad (19)$$

a considerable change of the pulse-shape occurs as now the resonant pulses are only partly covered by the sampling volume. The height of the pulse diminishes. The maximum signal can be roughly evaluated as

$$P(\Delta\theta/2\pi) \ln[(\Delta\phi/2\pi)(T/\Delta T)] \quad (20)$$

At even larger values of mismatch,

$$\Delta T/T > \Delta\phi/2\pi \quad (21)$$

the pulses cross the observation window separately, and the resonant phenomenon can hardly be detected. An example of the described behaviour is shown in Fig.8.

A possible way of identifying the existence of resonance experimentally, could be the sweep in the pulse period T from one pack of the pulses to another¹ and recording dependence of the pulse amplitude on the mismatch ΔT . If one defines the width ΔT_{res} of thus obtained resonant curve as a mismatch at which the signal becomes two times smaller than its maximum value, then, from Eqs.(14) and (20) one finds the following expression for ΔT_{res} :

$$\Delta T_{res}/T \sim \Delta\phi/2\pi\sqrt{N} . \quad (22)$$

To find the dependence of the signals on the position of the sampling volume (in case when it is displaced in a way that it does not any more intersect the resonant field line $\phi = \theta$, see Fig.4c,d) we consider dependences ϕ versus θ for different injection pulses near the point $\phi = \theta = \theta_0$. Since the vicinity of this point corresponds to small deviations of radius r from the resonant value $r = r_0$ ($r = r_0 + \xi$, with $\xi \ll r$), to obtain a curve corresponding to the last injected pulse, we can use the expansions

$$\begin{aligned} \theta - \theta_0 &= \Omega' \xi \bar{t} + \frac{1}{2} \Omega'' \xi^2 \bar{t} \\ \phi - \theta_0 &= \omega' \xi \bar{t} + \frac{1}{2} \omega'' \xi^2 \bar{t} \end{aligned} \quad (23)$$

with $\theta_0 = \Omega_0 \bar{t}$, where \bar{t} is the time elapsed since injection of this last pulse. Simple calculations show that, up to the terms quadratic in $\theta - \theta_0$, the following relation holds

$$\phi - \theta_0 = \frac{\omega'}{\Omega'} (\theta - \theta_0) + \frac{(\theta - \theta_0)^2}{2\bar{t}} \left(\frac{\omega''}{\Omega'^2} - \frac{\omega' \Omega''}{\Omega'^3} \right). \quad (24)$$

For the earlier pulses, one should replace \bar{t} by $\bar{t} + kT$, with $k = 1, \dots, N-1$, and $k = N-1$ corresponding to the first injected pulse (we assume that \bar{t} is not too small, $\bar{t} \gtrsim T/2$).

¹ The other option would be to keep T constant but rather sweep the particle energy (of course, keeping it constant within one pack). This is identical to sweeping in T_{mn} .

Let us denote the separation between the line-of-sight and the resonant line by ϕ_s . Then, assuming that $\omega'/\Omega' \sim 1$, and $\omega''/\Omega'^2 T \sim \Omega''/\Omega'^2 T \sim 1$, we conclude that in order all the pulses to be simultaneously covered by the sampling volume, the condition

$$\phi_s < (\Delta\phi)^{1/2} \quad (25)$$

should be satisfied. If, on the contrary, the condition

$$\phi_s > (\Delta\phi)^{1/2} \quad (26)$$

is satisfied, the last few injected pulses manifest themselves separately, and only the pulses with numbers less than $N - k$, with $k \sim \phi_s/\Delta\phi$, can be covered by the sampling volume simultaneously. The appearance of pre- (or post-) pulses can be taken as the criterion of the spatial resolution. This means that the localisation of the resonant field line can be made with the spatial accuracy of $a(\Delta\phi)^{1/2}$.

2.7 Detection of signals by means of a gate technique

The periodicity of the relevant signals makes it convenient to perform the analysis by means of well-known temporal integration techniques, which allow a sharper determination of the resonances. We consider here the use of a temporal gate technique, in which the monitoring system is open at given intervals of time and the detected signals are summed up. In this case, a pulsed target beam with characteristics similar to those of the injection beam can be used (see. Sec. 6). Electronics means are also possible. For a given sampling volume, as defined in Sec. 2.3, the temporal gate is characterized by the following parameters: the time T_{0G} of the first opening of the gate, the period T_G , the opening interval in each period τ_G , and the number N_G of the temporal windows of the gate. Thus, the signal is integrated over the following time intervals

$$T_{0G} + k T_G \leq t \leq T_{0G} + k T_G + \tau_G, \quad k = 0, 1, \dots, N_G. \quad (27)$$

To detect the resonances we take T_G equal to the injection period T , and sweep T as mentioned in Sec. 2.4. The time interval τ_G is assumed to be a given fraction of T . The general pattern of the signal is shown in Fig.9 as a function of T . This refers to a sampling volume located at the same toroidal position of the injection, i.e., in $\theta = 0$, and with $T_{0G} = 0$. From the figure different rational resonances can be identified. A toroidal displacement of the sampling volume allows the investigation of particular sets of resonances. The resonance pattern relevant to $\theta = \pi$ is shown in Fig.10, which refers to the same conditions of Fig.9, with $T_{0G} = 0.5 T$. It is apparent the disappearance of the peak corresponding to the $q = 2$ resonance. It is clear that, by changing the delay time T_{0G} , the appearance of resonance peaks can be also analyzed. As an example, the signal around the $q = 1$ resonance is shown in Fig.11, which refers to $\theta = \pi$, for the cases $T_{0G} = 0.5 T$, (exact resonance) and $T_{0G} = 0$.

3. ROLE OF THE FINITE BRIGHTNESS OF THE BEAM

3.1 Effect of a finite pulse-length

For the conditions of exact resonance ($\Delta T = 0$), the finite pulse-length will have no effect on the amplitude of the resonant pulse, as soon as the condition

$$\tau < T \Delta\phi / 2\pi \quad (28)$$

is satisfied. At larger pulse-lengths, the azimuthal length of the resonant bunch becomes larger than $\Delta\phi$, so that the sampling volume can simultaneously contain only a part of the pulse. Correspondingly, the pulse-length increases from $T\Delta\phi/2\pi$ to τ and the amplitude of the pulse decreases: expression (14) should be multiplied by $T\Delta\phi/2\pi\tau$. At the same time, increase of τ to the values exceeding $T\Delta\phi/2\pi$ will have no considerable effect on the background signal (16) caused by nonresonant particles. So, we come to the conclusion that, in order to provide good conditions for observing the resonant pulses, one should keep τ within the limits determined by Eq.(28). The modifications introduced by the finite pulse length in the resonance pattern obtained by a gate technique are shown in Fig.12, which refers to the $q = 1$ peak. The case of instant pulses and three

different pulse lengths τ have been considered. No appreciable variation with respect to the case $\tau = 0$ can be observed when the condition (28) is satisfied.

3.2 Effect of the beam velocity spread

The rotation frequencies Ω and ω of the fast particles scale as v . This means that scatter in v is roughly equivalent to the introduction of the frequency mismatch discussed in Sec.2.6. We have found that the characteristic width of the resonance ΔT_{res} is determined by the Eq.(22). So, for a rough estimate of the tolerable level of velocity spread that would not yet broaden the resonance, we should use the inequality

$$\Delta v/v < \Delta T_{res}/T \quad (29)$$

The effect of velocity spread of fast ions on the signals is illustrated in Fig.13, (referring as Fig.12 to the $q = 1$ resonance), where the signals corresponding to different values of $\Delta v/v$ are compared. It is apparent that velocity spreads satisfying the condition (29) produce only a slight decrease of the signal (with respect to the $\Delta v = 0$ case), which maintains its full detectability, while large velocity spreads lead to the disappearance of the resonant peak.

3.3 Effect of the finite beam width

We assume that the initial pulsed beam has a square cross-section of the size $b \times b$, with b much smaller than the plasma radius a . In a large aspect ratio tokamak, the angular width of the imprint of such a beam on plasma surface is much larger in a poloidal direction (b/r) than in a toroidal one (b/R). From our previous considerations (see Sec.2.3) it is clear that the effect of the final poloidal angular width will play no role in the detection of the signals, if it is smaller than the poloidal angular width of the observation volume (η/r), i.e., if the condition

$$b < \eta \quad (30)$$

is satisfied. At larger b , the signal from the observation volume will decrease as η/b .

At finite transverse dimensions of the neutral beam, the volume density of the trapped ions becomes also finite (for the needle-like neutral beam it was infinite, though the number of particles per unit length, that determines the amplitude of the observed signals remained finite). At the moment just after the injection of the neutral beam, the trapped particles occupy a volume of order of ab^2 and have a volume density of order P/ab^2 . Since the Jacobian $D(r, \theta, \phi)/D(r_0, \theta_0, \phi_0)$ of the transform (9) is equal to unity, the volume density of the trapped particles will remain constant at any time. The size of the beam imprint on every magnetic surface also remains constant, as is clearly seen from the transform (9). Then, as the length of the initial stretch (10a) occupied by the fast ions grows with time, this means that the size of the bunch across the magnetic surface decreases with time (approximately, as $1/t$ at not-too-small t 's). So, every bunch of fast particles acquires (with time) a belt-like shape, with the "height" of order of b , and thickness b' of order of abT/Lt . Clearly, at not very small t 's, b' is much smaller than b which, in turn is much smaller than the length of the bunch. This is the reason for our choice of the word "tagliatella" for the name of the resonant bunch.

The spatial structure of the stack of the bunches of the fast particles obtained in the conditions of the exact resonance, can be described as follows. The transverse cross-section of the stack just in the point of resonance ($r = r_0, \theta = \phi = \Omega t$) consists of the overlapping rectangles of identical height b and the width b' (the smaller the earlier the pulse has been injected). The density is maximum in the centre (where, after the injection of the N -th pulse it is approximately N times higher than for the single pulse) and decreases in the direction across the magnetic surface. It becomes two times less than in the maximum at the distance of approximately $2ab/NL$ from the centre. In the direction along the tagliatella the maximum density decreases because the "belts" originating from different pulses gradually diverge with a growing distance from the resonant point. Note that the direction along the belt does not coincide with that along any of the magnetic field lines (Cf. Fig.4a). According to Eq.(24), after the injection of the last pulse, i.e., at $t - NT \simeq T/2$, at the angular distance ϕ from the point $\theta = \phi$, the separation

of the "belts" corresponding to different pulses from the belt produced by the first pulse is approximately equal to $a\phi^2/(k+1)$, where k corresponds to the $(N-k)$ -th pulse. The density per unit length of the "stack" of the belts decreases for this reason when moving along the stack. The maximum density per unit length scales as $\ln N$, and decreases by a factor of two with respect to this level when only $N - \sqrt{N}$ pulses are stacked together (i.e., $k = \sqrt{N}$). Then, from the equation $b = a\phi^2/\sqrt{N}$, we find the angular distance on which the density per unit length decreases by a factor of two: $\phi \sim (b/a)^{1/2} N^{1/4}$. Therefore, the resonant bunch has a rather large size in the longitudinal direction.

If the pulse-length τ exceeds b/v_{\parallel} , then the initial length of the bunch of fast particles along the field-line is $b + v_{\parallel}\tau$. Accordingly, the volume density of the fast particles is reduced: it equals roughly $P/ab(b + v_{\parallel}\tau)$.

One more effect that should be taken into account for the neutral beam of finite transverse dimensions is a possible dependence of the frequencies Ω and ω on the angular co-ordinates ϕ and θ of the trapping point. This dependence appears due to the fact that the parallel (with respect to the magnetic field, Cf. Sec.2.1) velocity of the ions depends on the azimuthal angle of the trapping point. For a large aspect ratio case this dependence is weak and can be neglected. For a small aspect ratio the presence of this dependence causes an effect analogous to the velocity spread of the beam. The corresponding constraint on the beam transverse dimension b can be obtained by replacing $\Delta v/v$ in the l.h.s. of inequality (29) by $(b/a)(d\omega/d\phi)/\omega$.

The minimum dimension of the tagliatella can be affected also by the effects of finite Larmor radius. As soon as b' , formally evaluated as baT/Lt , becomes less than ρ_i , the further compression ceases, and the minimum dimension remains on the level of ρ_i . In this latter case the particle density in the tagliatella decreases correspondingly.

4. TOROIDAL EFFECTS

In the model of a cylindrical tokamak that we have discussed in the previous sections, the magnetic field does not vary along the field line, so that at even very small values of v_{\parallel} the ions can encircle the magnetic axis. In the toroidal geometry, in order to

avoid the toroidal trapping, one should inject the neutrals at an angle that is not too close to 90° with respect to the magnetic field. This imposes some constraints on geometry of the conceivable experiment.

On the other hand, the effect of the toroidal trapping can be used to deliberately create a population of ions bouncing between their turning points in some region of a tokamak and to employ the resonance between the bouncing frequency and the frequency of the neutral beam pulses to produce a high density bunch of ions on a certain field-line. The spatial structure of this object will be quite similar to that of the "tagliatella" described above, with relatively large length, medium width and small thickness.

What will be considerably different in this case, is a reaction of the resonance to the drift motion of the fast ions, in particular, to the one caused by the radial electric field. Indeed, in the case of the transit ions, unless they are very close to the trapping boundary, the electric field would cause just some minor change in the rotation frequency of the ions around the magnetic axis, with a corresponding minor change in the resonant frequency. On the contrary, in the case of the trapped ions, the drifts would move the ions out from the field line onto which they have been injected, and the time of stacking would be shortened. Detailed considerations of this effect which has clear diagnostics implications will be published elsewhere.

5. PARAMETERS OF A CONCEIVABLE EXPERIMENT

In order to better understand whether the experimental detection of the effects discussed in our paper is really possible, we consider a numerical example related to the conceivable experiment on a medium-size tokamak.

Let's assume that the neutral beam with a pulse-length of $0.3 \mu s$ is composed of deuterons, has a current of $100 A$ and an energy of $80 keV$. For a plasma with density of $5 \times 10^{13} cm^{-3}$ and temperature of a few keV this would correspond to a penetration length of approximately $1 m$. The distance between bunches of $10 \mu s$ would correspond to the length of the magnetic field line of $10 - 20 m$, depending on the injection angle.

For the total number of pulses in the pack equal to 20, the pack duration would be $200 \mu s$. Even for the continuous beam with the aforementioned parameters the energy content in the pack would not exceed $1.6 kJ$. The desirable energy spread of approximately 2% is rather demanding but could, probably, be assured for the beam of a relatively short pulse-length, just by cutting it out from much longer quasicontinuous beam.

For the pulse-length of $0.3 \mu s$, the length of the initially formed bunch of fast ions along the field lines is approximately $30-50 cm$. This means that the size of the beam in this direction can be relatively large, up to a few tens of cm , without any negative effect on the overall performance of the system. We take a value of $30 cm$ for it.

For the beam size across the field lines, we assume a value of $10 cm$. With the choice of parameters given above, the beam current density would not exceed $0.3 A/cm^2$, well within the presently achieved values.

As it has been already pointed out, the just trapped single bunch of the fast ions will occupy a region with the dimensions approximately equal to $60 cm$ along the field lines, $100 cm$ along the radius, and $10 cm$ across the two other dimensions. As the total number of particles in $0.3 \mu s$, $100 A$ pulse is 2×10^{14} , the number density in the bunch will be approximately $3 \times 10^9 cm^{-3}$. The maximum density in the point of exact resonance will be 20 times larger (as far as the minimum dimension of the tagliatella exceeds the gyroradius ρ_i of the fast ions; if the formally evaluated b' is less than ρ_i , then the volume of the tagliatella should be evaluated as $Lv\tau\rho_i$, with the corresponding reduction of the particle density). As the energy of the ions constituting the tagliatella is an order of magnitude higher than the ion temperature, the relative pressure perturbation is 10 times larger than the relative density perturbation, and may reach 10%. In this respect, the tagliatella may be of some interest as a tool that can be used to affect the plasma behaviour near the resonant surfaces.

As it has been already mentioned, to detect the resonant bunch, one can use a special "target" beam, crossing the plasma in the desired cross-section. We assume the target beam to have parameters similar to the ones of the initial beam, in particular, the cross-section of approximately $250 cm^2$; in the case of the target beam we, however, as-

sume that the target beam has a square cross-section ($16 \times 16 \text{ cm}^2$), i.e., $\eta = 16 \text{ cm}$. With the current density of 0.4 A/cm^2 , the density n_A of the neutral atoms in the beam is approximately 10^{10} cm^{-3} .

According to the results of Section 2.5, for the pulse-length of $0.3 \mu\text{s}$, the duration of the signal on the monitor will be also approximately $0.3 \mu\text{s}$. The number of fast ions that are simultaneously present in the sampling volume, when it is covered by the central part of the resonant tagliatella, is (see Sec.3.1)

$$P \ln N \frac{\eta}{L} \frac{\eta}{v_{\parallel} \tau}. \quad (31)$$

In order to find the number of charge-exchange neutrals produced per unit time, this number should be multiplied by $n_A \sigma_{cx} v$, where σ_{cx} is the charge-exchange cross-section. Multiplying this product by the pulse-length τ , we find the total number of charge-exchange neutrals p' produced during the single traverse of the central part of the tagliatella through the target beam:

$$p' = P \ln N \frac{\eta}{L} \frac{v}{v_{\parallel}} \eta n_A \sigma_{cx}. \quad (32)$$

The secondary charge-exchange and the ionization of the thus produced fast atoms reduces their number approximately by a factor of 2. Substituting all the numerical values given above, we find that the number of fast atoms that is produced during one pulse is $p' \simeq 10^9$. Their detection on the background of other charge exchange particles should be facilitated by the fact that they have a well defined energy and escape from every point of the plasma along the conical surface determined by their pitch-angle (which is also well defined).

Some additional advantages can be gained in the case when the aforementioned technique is applied for the studies of the magnetic field structure and/or fluctuating fields near the separatrix of tokamaks with divertor. Here the pulsed beam can be injected tangentially, near the upper point of the poloidal cross-section (see Fig.14), while

the detection can be made near the X-point, where the density of trapped ions should increase because of their long residence time near this point. As the plasma temperature in the periphery of the tokamak is relatively low, one can use the injection of NB of heavier atoms (like lithium), which will not be completely stripped, so that the optical monitoring would become possible /8/. This would allow to increase the overall sensitivity of the diagnostic.

6. CONCLUSIONS

We have shown that, by the pulse-periodic injection of the neutral beam into a tokamak plasma, resonant bunches of fast ions can be formed near the rational magnetic surfaces. To create such a bunch, one should adjust the time-distance between two successive pulses of the neutral beam and the rotation period of fast ion along the closed magnetic field line.

The spatial structure of the resonant bunch is characterized by a rather large longitudinal extent, and a strong difference in the two other dimensions. Because of this very characteristic form of the bunch we propose to call it "tagliatella".

With existing or slightly developed neutral beam technique, one can produce tagliatelle with maximum density of fast ions of order of a few percent of plasma density, and the pressure up to 10% of plasma pressure. Detection of resonant tagliatelle can be used for the investigation of the magnetic field structure (in particular the magnetic islands), and of the collective interaction of fast ions with fluctuations. The diagnostics based on the pulse-periodic injection of the neutral beams can be used also for the studies of the regions near the separatrix in tokamaks with divertors.

The resonance phenomena described in our paper should exist also in other types of the toroidal devices, like reversed field pinches and stellarators.

7. ACKNOWLEDGEMENT

One of the authors (D.R.) is grateful to the Istituto di Fisica del Plasma, C.N.R., for its hospitality in the course of this work.

APPENDIX 1

Injection of infinitely short neutral beam pulses into a cylindrical tokamak

We consider the injection of a neutral beam pulse in the equatorial plane of the tokamak. If time and the toroidal angle are counted respectively from the moment and the place at which the bunch crosses the tokamak boundary (at $r = a$), then the crossing of the magnetic surface of a radius r occurs at the moment $(a - r)/v \sin \alpha$ at the toroidal angle $\theta_0 = (a - r)/R \cot \alpha$. The ions trapped at this surface have rotation frequencies $\Omega(r)$ and $\omega(r)$ determined by Eqs. (7), and (8). They move along the field line according to Eqs.(9):

$$\begin{aligned}\theta &= \frac{a-r}{R} \cot \alpha + \Omega(r) \left(t - \frac{a-r}{v} \sin \alpha \right) \\ \phi &= \omega(r) \left(t - \frac{a-r}{v} \sin \alpha \right)\end{aligned}\tag{A1.1}$$

At the moment $t = a/v \sin \alpha$ when the neutral beam bunch crosses the magnetic axis, the ions occupy the line that is defined by the equations:

$$\begin{aligned}\theta &= \frac{a}{R} \cot \alpha - \frac{r}{R} \frac{r^2}{r^2 + q^2 R^2} \cot \alpha \\ \phi &= \frac{r}{qR} \frac{\cot \alpha}{1 + r^2/q^2 R^2}\end{aligned}\tag{A1.2}$$

For a large aspect ratio tokamak, $R \gg a$, all the ions have small values of ϕ and essentially the same values of θ . Note that, numerically, even for a relatively small aspect ratio of two, the stretch that is being initially occupied by the ions differs only very little from the straight segment determined by Eq. (10a). The subsequent bunches occupy initially the same line so that no accumulated phase shifts arise from the finite flight time and oblique injection.

APPENDIX 2

Stretching of the bunch of fast ions

Let $f(r)$ be the function that describes the line-density of the ions just trapped after injection of the NB pulse:

$$dP = Pf(r)dr \quad (A2.1)$$

with P being the total number of particles trapped at the stretch $0 < r < a$, dP the number of particles trapped within the interval $(r, r + dr)$. It is implied that f is normalized to unit:

$$\int_0^{\infty} f(r) dr = 1 \quad (A2.2)$$

The initial interval of the length dr is being stretched in the course of the particle motion along the field lines. At time t , the points r and $r + dr$ will move to their new angular positions,

$$\phi = \omega(r)t, \quad \theta = \Omega(r)t, \quad (A2.3)$$

and

$$\phi + d\phi = (\omega(r) + \omega'(r)dr)t, \quad \theta + d\theta = (\Omega(r) + \Omega'(r)dr)t, \quad (A2.4)$$

respectively. The distance between the ends of the interval is, obviously,

$$dr \left[1 + (\omega' r)^2 t^2 + (\Omega' R)^2 t^2 \right]^{1/2}, \quad (A2.5)$$

so that the initial line density at radius r is transformed to:

$$Pf(r) \left[1 + (\omega' r)^2 t^2 + (\Omega' R)^2 t^2 \right]^{-1/2}, \quad (A2.6)$$

At not-too small t ,

$$t > (r/R)T \quad (A2.7)$$

it evolves as $1/t$.

At the resonant surface, the pulses are added to each other with the time-shift T . If the time after injection of the last ($N - \text{th}$) pulse satisfies the condition (A2.7), the linear density in the resonant point is, clearly, the following:

$$\frac{P f(r)}{[(\omega' r)^2 t^2 + (\Omega' R)^2 t^2]^{1/2}} \sum_{l=0}^{N-1} \frac{1}{t - lT} \quad (A2.8)$$

(note that here t is larger than $(N - 1)T$). If N is large and the time $\bar{t} = t - (N - 1)T$ elapsed since injection of the last pulse is large enough, $\bar{t}' > T/2$, then a simple asymptotic expression is valid:

$$\sum_{k=0}^{N-1} \frac{1}{t - kT} \approx \frac{1}{T} \ln\left(\frac{N}{\bar{t}/T}\right). \quad (A2.9)$$

This asymptotics breaks down at $\bar{t} \sim NT$; at even larger \bar{t} , the sum is approximately equal to N/\bar{t} .

REFERENCES

- /1/ A. I. Kislyakov, in *Diagnostics for Contemporary Fusion Experiments*, Proc. of the International School of Plasma Physics (P.E.Stott et al - Eds), Editrice Compositori, Bologna, 1992, p.455.
- /2/ S. Corti, G. Bracco, A. Moleti, V. Zanza, A. V. Khudoleev, A. I. Kislyakov, M. P. Petrov,, and S. Ya. Petrov, *Diagnostics for Contemporary Fusion Experiments*, Proc. of the International School of Plasma Physics (P.E.Stott et al - Eds), Editrice Compositori, Bologna, 1992, p.477.
- /3/ A. Weller, A. D. Cheetham, A. W. Edwards, R. D. Gill, A. Gondhalekar, R. S. Granetz, *Phys. Rev. Lett.* **30**, 2303 (1987).
- /4/ F. C. Jobs, in *High-Temperature Plasma Diagnostics*, Proc. of the 2nd Topical Conference, Santa Fe, 1978, LA-7160-C, 101.
- /5/ V. I. Afanas'ev, A. I. Kislyakov, S. V. Lebedev, S. Ya. Petrov, F. V. Chernyshev, K. G. Shakhovets, *JETP Lett.*, **50**, 485 (1989).
- /6/ J. D. Callen, "Models of Plasma Confinement and Heating in Tokamaks", University of Wisconsin Plasma Report UWPR 89-2, 1989.
- /7/ J. O'Rourke, J. Blum, J. G. Cordey, A. Edwards, N. Gottardi, B. Keegan, E. Lazzaro, G. Magyar, Y. Stephan, P. Stubberfield, D. Veron, and D. Zasche, in *Controlled Fusion and Plasma Heating*, Proc. of the 15th European Conference , Dubrovnik, 1988, (European Physical Society, 1988), vol 12B, Part I, 155.
- /8/ P. C. Stangeby, G. M. Mc Cracken, *Nucl. Fus.* **30**, 1225 (1990).

FIGURE CAPTIONS

Fig. 1 Periodically pulsed neutral beam; I_{NB} is an equivalent current, N is the total number of pulses in the pack, τ is the pulse length, and T the pulse period.

Fig. 2 Cylindrical model of a tokamak. The neutral beam is injected in the (xz) plane, and aimed to the device axis.

Fig. 3 Plot of the model dependences of q , Ω , and ω vs r (curves a, b, c respectively). The safety factor q is lower than 1 on the axis and larger than 1 at the plasma periphery. The intersection point of curves b and c corresponds to the $q = 1$ surface.

Fig. 4 Evolution of the system in the (θ, ϕ) plane. (A) Shape of the stretch (10a) at different times. Curves a, b, c, d, e refer to $t/T = 0.2, 0.4, 0.6, 0.8,$ and $1,$ respectively. The dashed curves correspond to $\theta = q(0)\phi$, and $\theta = q(a)\phi$, and the dotted curve to $\theta = \phi$ (i.e., to $q = 1$). (B) Shape of the stretch (10a) at large time $t = 25T$. (C) Superposition of two bunches (injected at $t = 0$ and $t = T_{11}$) at $t = 1.5T$. The dashed curve corresponds to the first bunch, and the dotted curve to the second bunch. The two squares correspond to two different sampling volumes: one is centered at $\theta = \phi = \pi$, while the other is shifted both in θ and ϕ . (D) Superposition of three bunches (injected at $t = 0, t = T_{11},$ and $t = 2T_{11}$) at $t = 2.5T$. The first bunch is represented by the continuous line, the second by the dashed curve, and the third by the dotted curve.

Fig. 5 Geometry of the sampling volume situated near the plane $z = z_0$.

Fig. 6 Time evolution of the signal for the case of $N = 1$ pulse at exact resonance for two different sizes of the sampling volume. Case A refers to $\eta = 0.1$, and case B to $\eta = 0.01$. The other parameters are $d = 0$, and $a_1 = 0.15a$ (see Secs.2.3 and 2.4).

Fig. 7 Time evolution of the signal S for $N = 20$ pulses at exact resonance. The parameters are $d = 0$, $\eta = 0.05$, and $a_1 = 0.15 a$.

Fig. 8 Time evolution of the signal S for $N = 20$ pulses at $\Delta T/T_{11} = 0.1$. The other parameters are the same as in Fig.7.

Fig. 9 Integrated signal (obtained by the gate technique) versus the injection period T normalized over T_{11} . The chosen parameters of the gate are $T_{0G} = 0$, $T_G = T$, $\tau_G = 0.04 T$, and $N_G = 21$. $N = 20$ pulses have been considered. The sampling volume is located at $\theta = 2\pi$. For the considered profiles of q and Ω the period of the $q = 2$ resonance is $T_{21} \simeq 3.06T_{11}$.

Fig.10 Same as in Fig.9 at $\theta = \pi$, for $T_{0G} = 0.5 T$.

Fig.11 Same as in Fig.10 for different values of the first opening of the gate. The continuous line refers to $T_{0G} = 0.5 T$, and the dotted line to $T_{0G} = 0$. Note the change of the horizontal scale.

Fig.12 Behavior of the integrated signal for different pulse lengths. Curves a, b, c refer to $\tau = 0.01, 0.05$, and 0.1 . The other parameters are the same as in Fig.10.

Fig.13 Behavior of the integrated signal for different velocity spread of the beam. Curves a, b, c, d refer to $\Delta v/v = 0, 0.01, 0.05$, and 0.1 . The other parameters are the same as in Fig.10.

Fig.14 Schematic of the experiment on the injection of a pulsed periodic beam to the peripheral plasma of the divertor tokamak. The peripheral plasma occupies the region between the separatrix and the dashed curves. The arrow shows the projection of the beam velocity on the plane of the figure. There exists also a velocity component parallel to the magnetic axis (perpendicular to the plane of the figure). The detection system could be situated in the vicinity of the X-point.

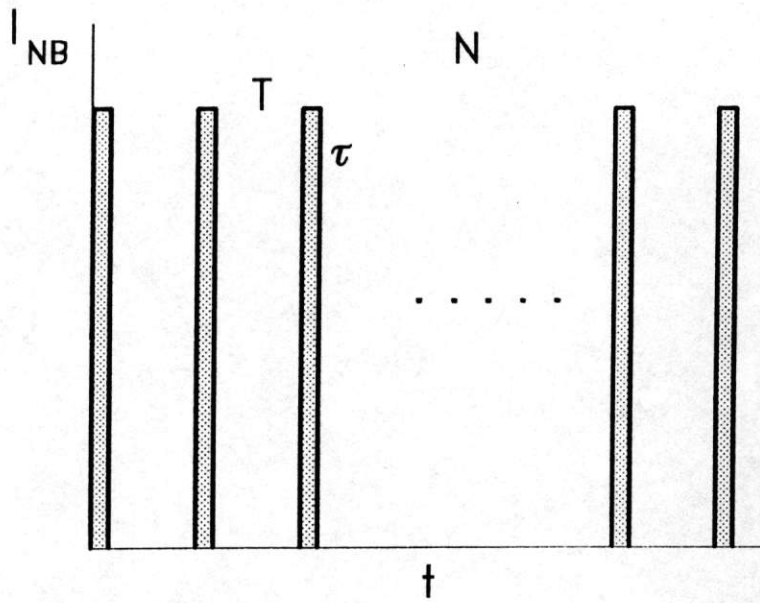


Figure 1

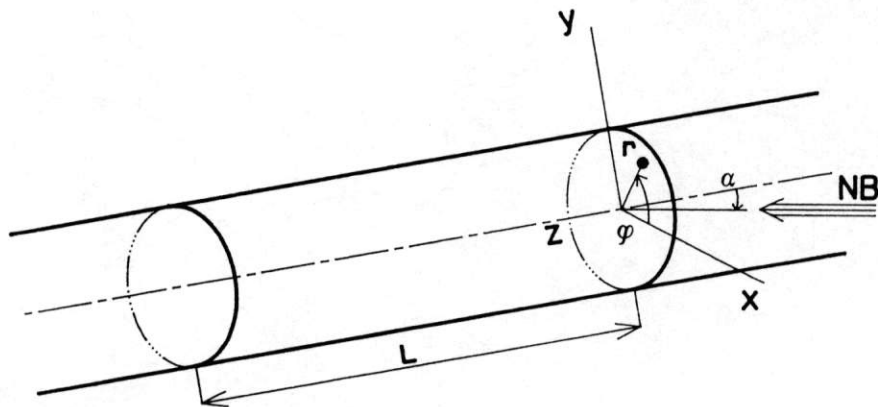


Figure 2

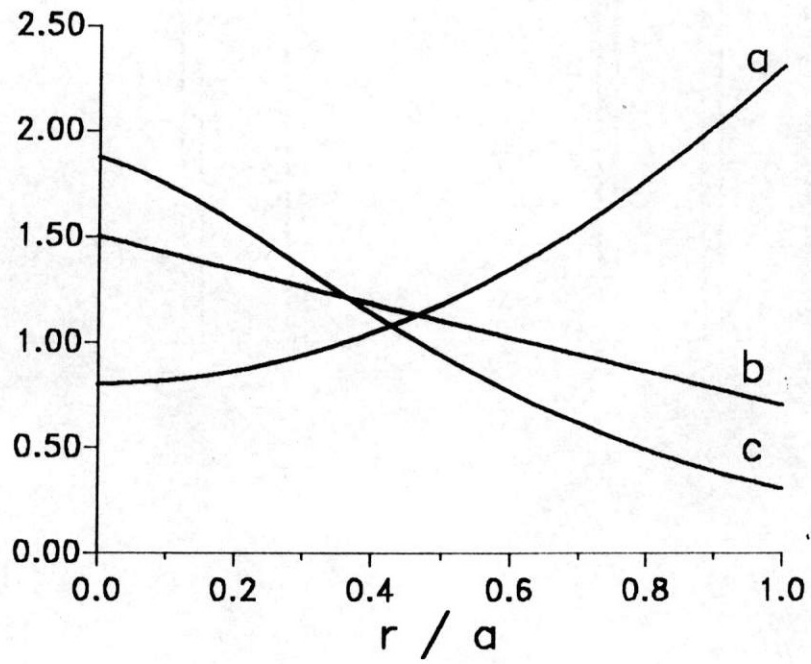


Figure 3

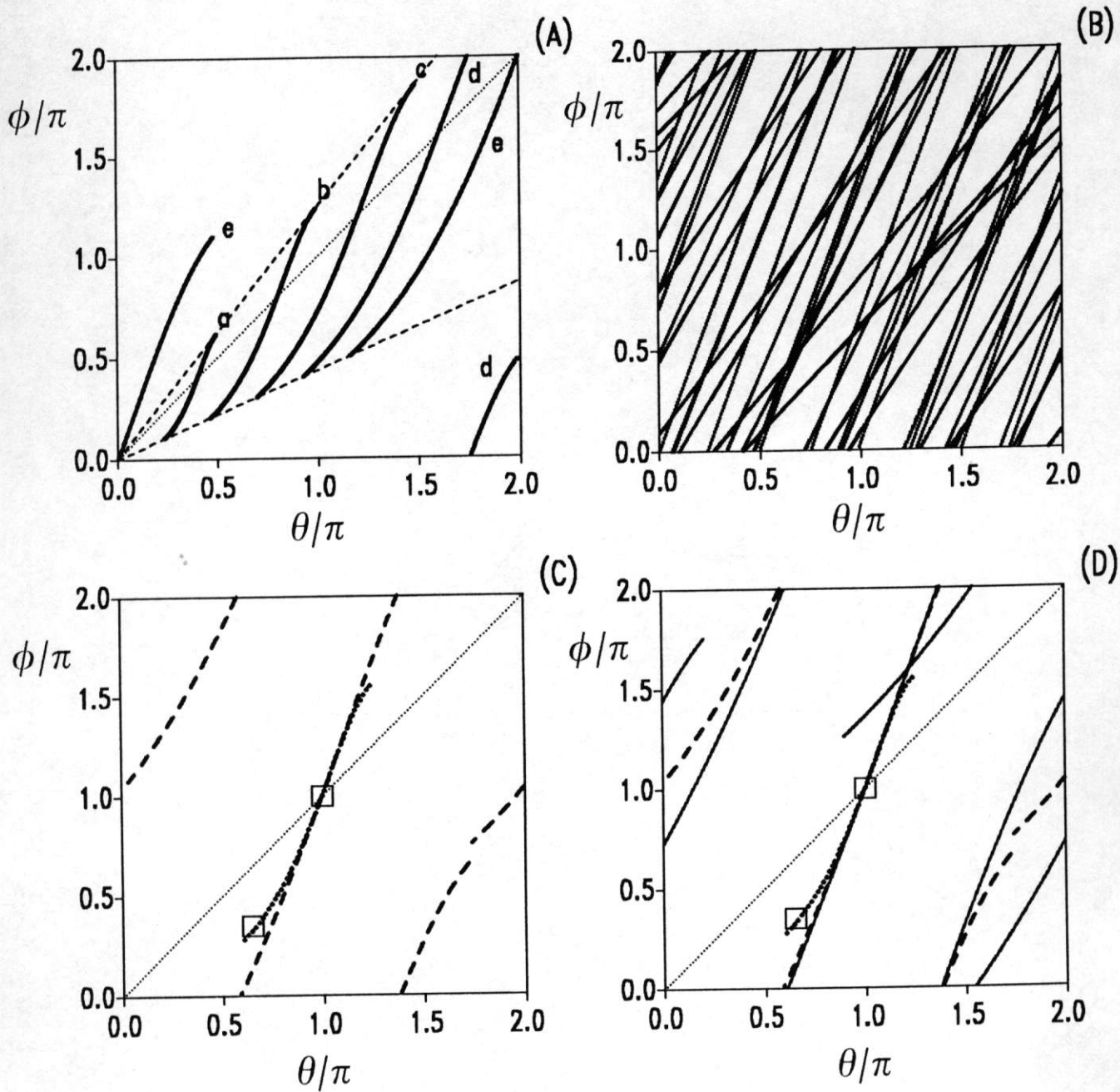


Figure 4

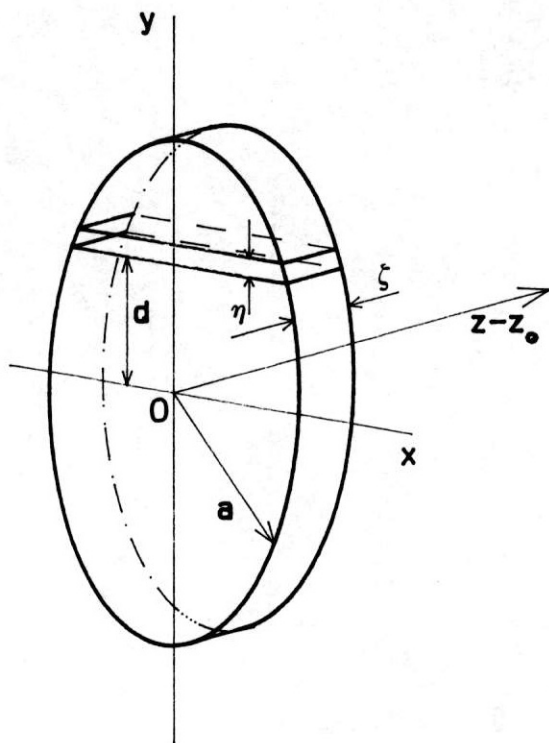


Figure 5

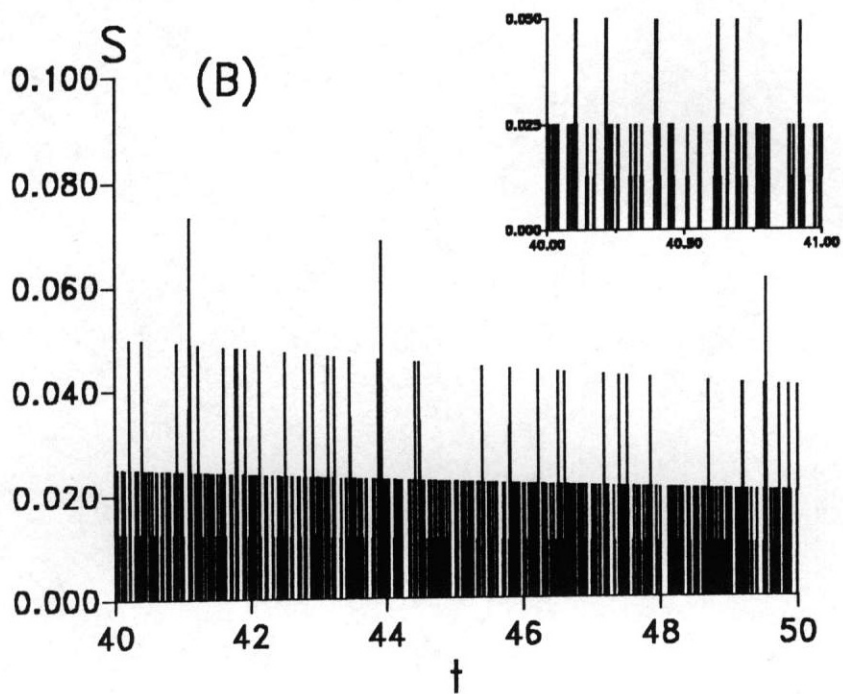
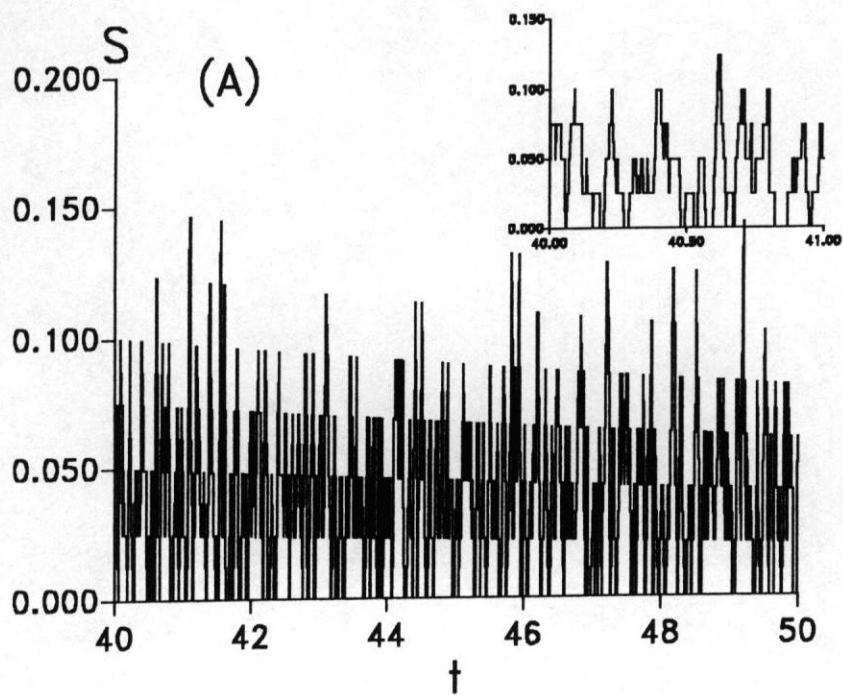


Figure 6

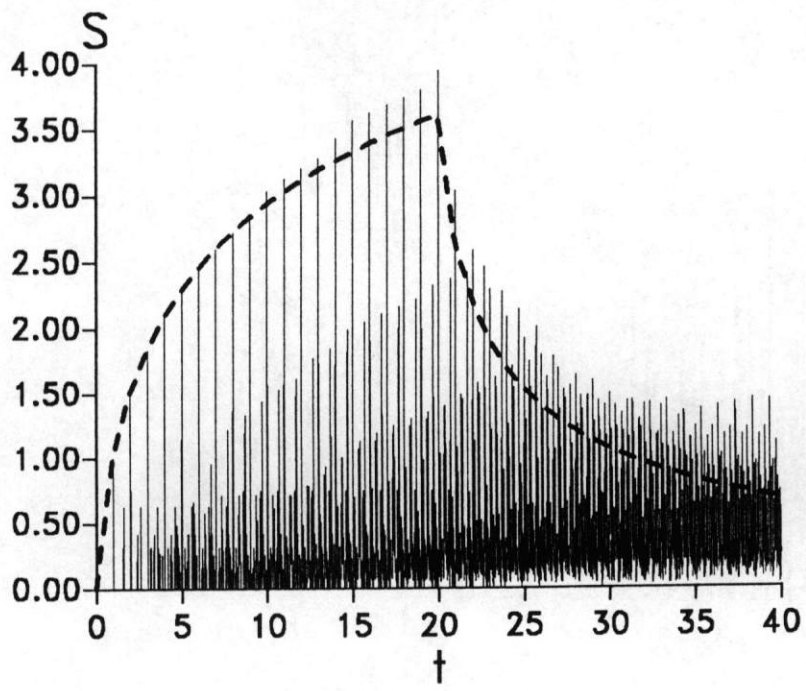


Figure 7

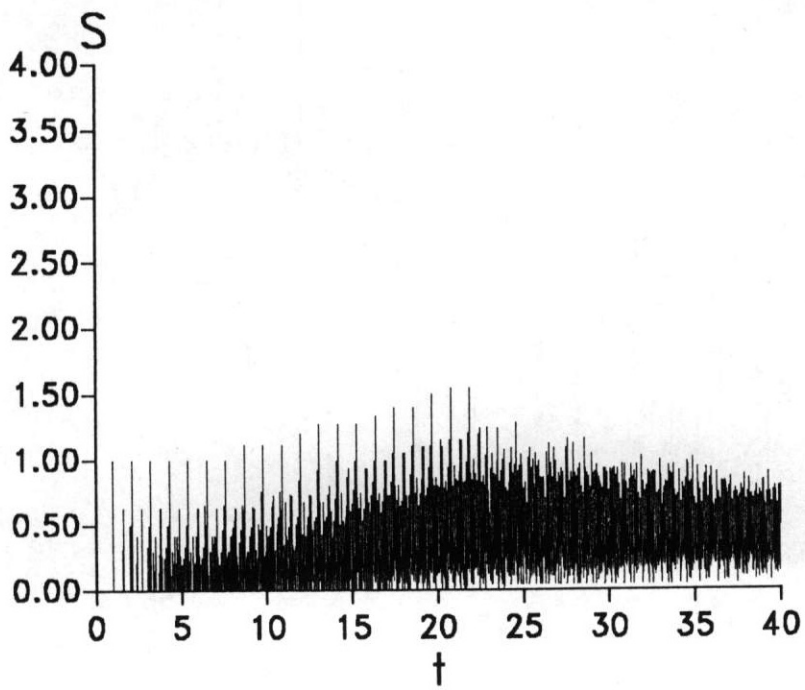


Figure 8

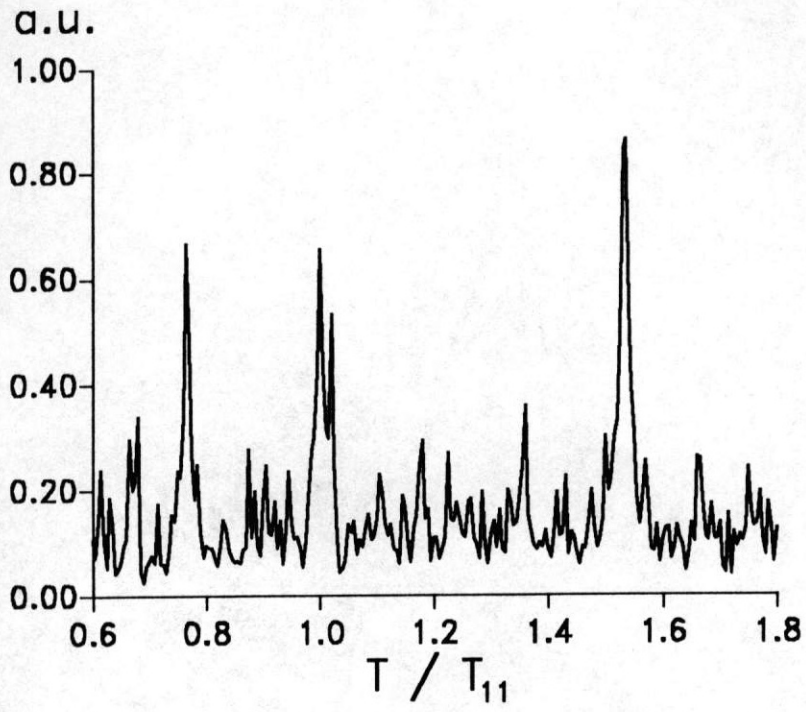


Figure 9

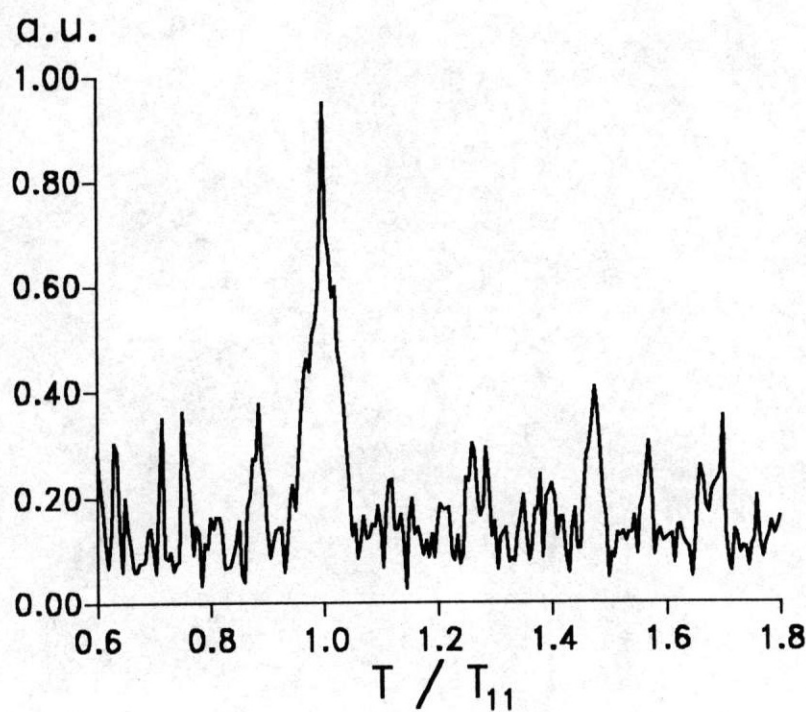


Figure 10

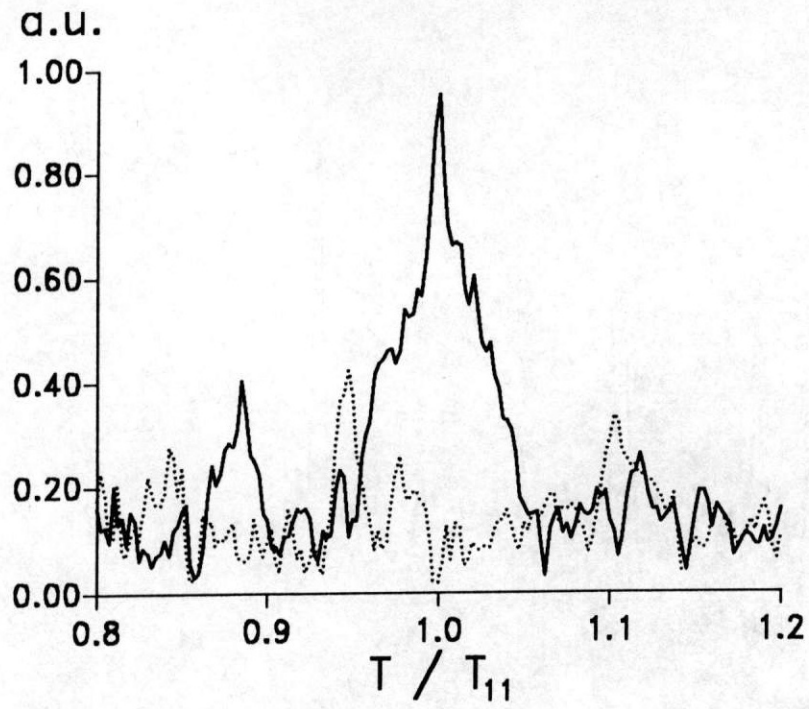


Figure 11

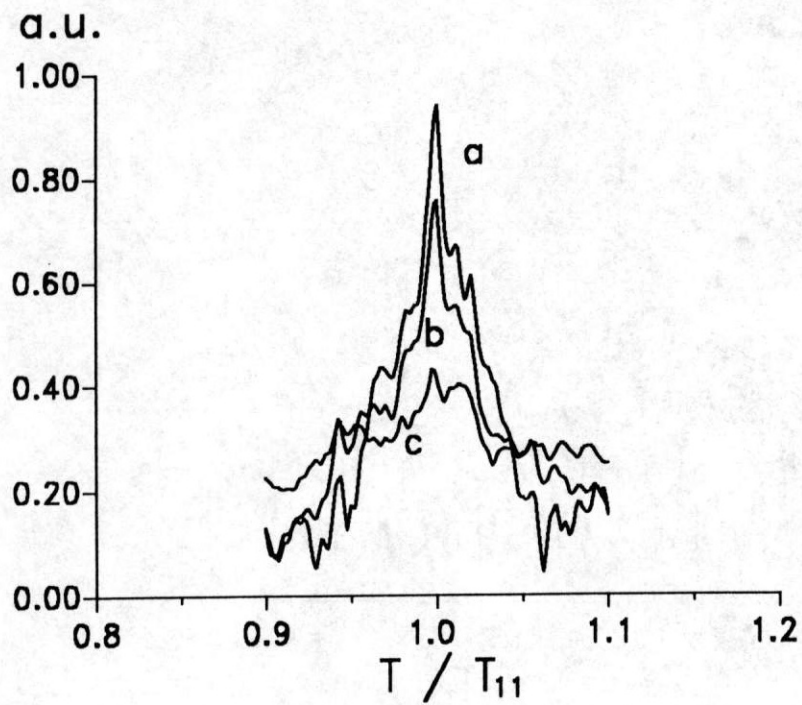


Figure 12

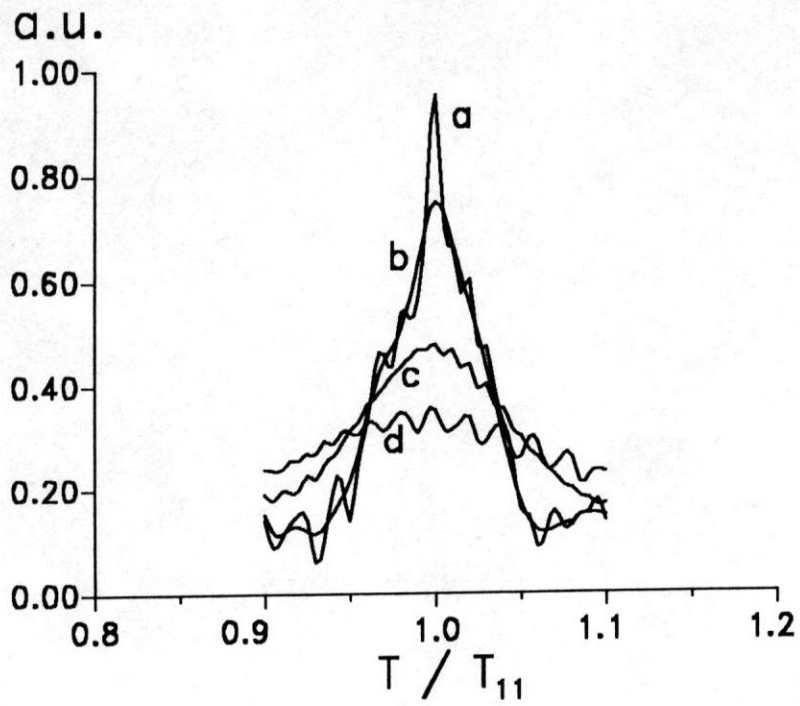


Figure 13

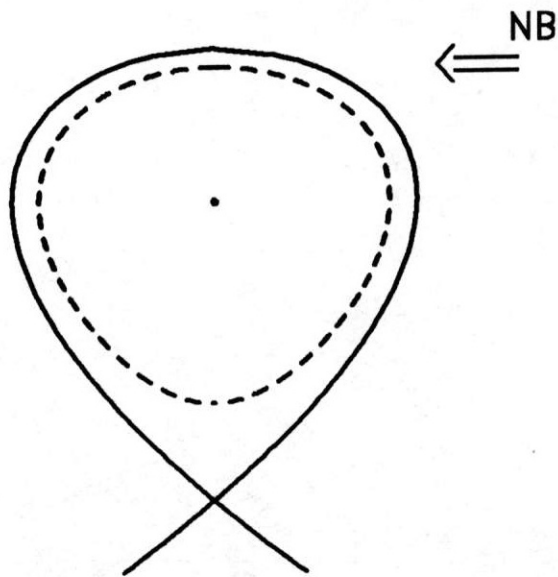


Figure 14